33RD CONGRESS
OF THE INTERNATIONAL COUNCIL
OF THE AERONAUTICAL SCIENCES
STOCKHOLM, SWEDEN, 4-9 SEPTEMBER, 2022

ICAS 2022 SWEDEN

INVESTIGATION ON INTEGRATING RECYCLABILITY AS A FUNCTION AT THE DESIGN PHASE OF COMPLEX-LOADED STRUCTURAL COMPONENTS

Angelos Filippatos[1,2,*], Kaushik Abhyankar[2] & Georgios Tzortzinis[1,2]

[1]Dresden Center for Intelligent Materials (DCIM), Technische Universität Dresden, 01069 Dresden, Germany
[2]Institute of Lightweight Engineering and Polymer Technology, Technische Universität Dresden, Holbeinstraße 3, 01307 Dresden, Germany

Abstract

We consider recycling as a complex, non-mechanical function during the design phase. We investigate the impact of substituting pristine with recycled fibers on the main structural function of a component by applying the function-oriented spiral development approach. The integration of the function is defined and included at the requirements and the design phase. Here, the recycling-as-a-function approach aims to design by meeting the recycling criteria, while considering its impact on the global stiffness and on the efforts for typical loading conditions of a hat-stiffener with skin.

Keywords: multi-material design, recycling, composites, sustainable design, gradient-free optimization

1. Introduction

The typical straightforward design approach in aerospace industry of the last 30 years is to select, combine and join different materials with the aim of optimizing mass, manufacturing performance and operation phase [1]. Especially, carbon fiber-reinforced polymers have succeeded to become the pioneer structural material in the aviation industry, as they combine remarkably lightweight and strength properties [2]. However, the increasing use of CFRPs in aviation industry also rises environmental concerns related to the waste treatment of these composites and their recycling capabilities [3, 4].

These concerns reflect our current societal challenges, especially resource scarcity and climate change and are summarized to the global societal objective to achieve climate neutrality to 2050. In a sense, recycling-as-a-challenge in society is reflected to the aeronautical community as recycling-as-a-function, pushing us to integrate recyclability into all lifecycle phases, from design and development, to manufacturing, operation and decommission. These societal challenges motivate the aeronautical community to define new goals and objectives to the multi-material design of aerostructures and try to achieve solutions with high recycling rates of the high-cost, energy-intensive carbon fibers of CFRPs [5].

The discussion whether recycling is relevant for the aerospace sector is still ongoing and different arguments are made based on the selected point of view. For example, some researchers are in favor, when comparing the material mix with other sectors, meaning that aerospace have a heavy energy mix of materials [6]. Other researchers, state that compared to the whole energy consumption across the whole lifetime of the product-airplane, recycling the materials is less relevant than the respective materials in other composite-heavy sectors, for example in the automotive and wind energy industry [5, 7]. Nevertheless, and apart on how this discussion evolves, research on recycling of composite components for the retrieval of the constituent materials, fibers and matrix is ongoing, with papers covering the chemical process [8] and the material characterization of the reduced mechanical properties of the fibers [9, 10].

To the authors' knowledge, there is little research on the area of designing using only recycled fibers (single-malt approach), or in a mix with pristine fibers (blended approach). Some results are shown to include fibers to non-structural components of an airplane, e.g. interior parts [11]. However, due to mainly open questions regarding consistency of mechanical properties of the recycled fibers [12], specifically undulation and fiber-length restriction [13], the relevant design results are scarce [14].

1.1 State of the art

Currently, conventional recycling methods allow decomposing the matrix and reclaiming the carbon fibers [8, 15]. Nevertheless, these techniques come at a cost in terms of mechanical properties of the fibers, especially to a wide strength degradation ranging up to 16% [16]. Even though more recent research efforts have managed to retain more than 90% of the original properties [17], a common practice is missing to reuse them in the aerospace industry, mainly due to a high scatter of the achieved properties and the regulations in aerospace industry of material certification. In an effort to reduce the environmental footprint associated to the manufacturing of new fibers, this work inspires to promote the sustainable design of aeronautical components by enabling a tailored **mix of recycled and pristine fibers** undergoing typical loading conditions.

Manufacturing methods to fabricate hybrid or mixed preforms and textiles are state of the art, some of them like the tailored fibre-placement (TFP) [18], automated tape placement and the braiding or filament winding method [19, 20] having already found their implementation in the aerospace industry. Having this in mind, we focus here on the design phase of a stiffened fiber-reinforced epoxy panel, and the arrangement of pristine and recycled fibers, while addressing the manufacturing conditions of the preforms and the challenges that arise from that.

The structural design of modern aircrafts requires stiffened fiber composite panels on the fuselage and wing structures. These panels typically consist of skin, ribs and T or hat-stiffeners, with the loads carried depending on their position along the aircraft. For relatively simple components, the VDI guideline 2221 [21] provides a long-tested and robust basis for an efficient approach. It fundamentally divides the design process into four serial phases, (i) clarifying and adaptation of the task, (ii) elaboration of the solution concept, (iii) designing the modules, and (iv) elaborating the details and verification. This principle has proven itself in practice and has been adopted by several authors for years. Moreover, the advanced application of composite components in the aerospace industry has led to considerable efforts to optimize their mechanical properties. In an early effort by Vitali et al [22], the pressurized upper cover panel of a passenger aircraft formed the basis for structural optimization of the geometric characteristics of the skin and stiffeners under varying loading conditions. Jin et al al [23] in a work with both experimental and computational aspects focused on the design sensitivities of relevant geometric parameters and provided a framework aspiring to reduce the time-to-market.

For the design of complex structures, investigations have driven developments that include "intelligent" approaches of combining simulations with optimization algorithms. For example, finite element analyses and optimization algorithms are combined to design composite lateral wing upper covers under axial compressive loads [24, 25]. In context of optimization algorithms, many researchers have used binary-representation-based genetic algorithm (GA) [26] for minimization of generic application-specific functions. This method was further developed [27, 28], with one of the main advantages compared to conventional methods is the absence of evaluating gradients of the objective function, which in some cases either it is computationally costly or not possible. Further binary representations have evolved to include a highly efficient uniform crossover operator, which is normally not applicable to permutation representations [29], with numerous practical implementations of this algorithm found in the literature [30]. Researchers have compared performances of genetic algorithms and gradient-based algorithms [31], concluding that the genetic algorithms require significantly more objective function evaluations, whereas gradient-based algorithms require tedious gradient-calculation routines. Depending on the nature of the problem, the number of design variables, and the degree of convergence, the GAs require more objective function evaluations, whereas gradient-based algorithms require tedious gradient-calculation routines. In the field of composite structures, due to the nature of complex objective functions to be optimized, many researchers have opted for GA instead of a gradient-based optimization algorithm.

Genetic algorithm is used to optimize ply thickness and orientation of composite structures [32]. In the field of structural health monitoring of composites, researchers [33] have accurately identified the impact load for a given composite structure using GAs. Some scientists have used GAs to optimize stacking sequence of composite laminates [34]. However, to the authors' knowledge there little or no research to spatially optimize single filaments inside each layer, specifically with a mixture of pristine and recycled fibers.

2. Materials and Methods

To demonstrate the efficiency and the potential of the proposed design methodology in integrating contradictory functionalities, we use as a demonstrator a composite hat-stiffener with skin. The goal is to conclude on the topologically and quantitatively optimal mix of pristine and recycled fibers, prioritizing as main functions, the structural function (structural integrity) and the recyclability of the examined components.

2.1 Materials

Composite stiffened panels are extensively used in aircrafts as they represent the design approach of meeting the high stiffness with minimal weight requirements, whereas the applied loads are depending on their position along the aircraft. In particular, the fuselage is typically subjected to bending during landing, while radial pressure is present due to the internal and external differential pressure. On the other hand, panels on the wings are subjected to in-plane axial compressive and shear loading emerging form the wing bending and torsion under aerodynamics loads [35]. In the framework of this work, the lay-up of the examined wing section has been obtained from [25] and simplified as illustrated at Figure 1.

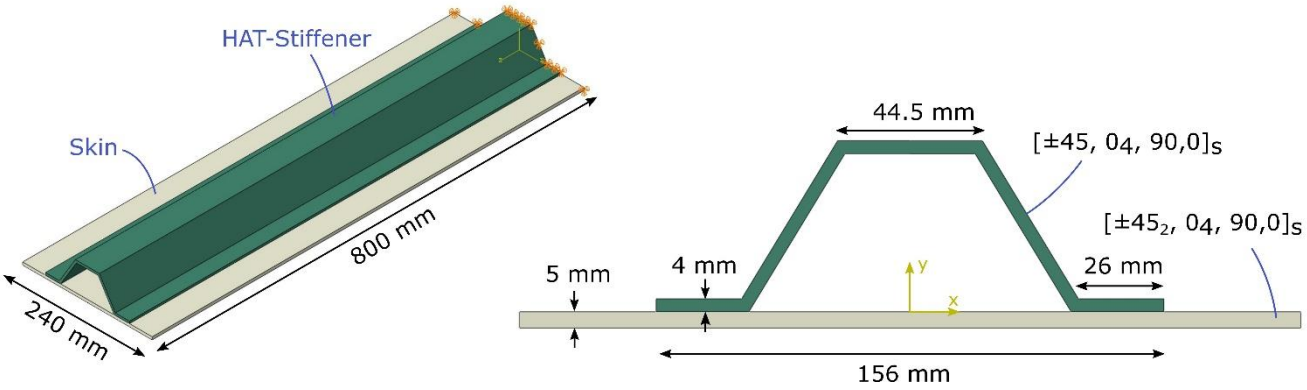

Figure 1 – Geometry of the skin with hat-stiffener with their dimensions, and lay-up.

For the numerical simulations we select typical composite materials for the aerospace industry. The ply properties were derived based on the rule of mixtures for pristine carbon fibers (CF) Tenax UMS 40 and aerospace grade epoxy. To account for the degradation of the mechanical properties of the recycled fibers, the elastic and shear modulus were reduced by 20% to reflect the experimental findings of [9]. For volume fraction 60% and 0.25 mm ply thickness the assumed properties are summarized in Table 1.

Table 1 - Mechanical properties of pristine and estimated recycled Tenax UMS 40 carbon fibers and the respective properties with aerospace grade epoxy from Altair ESAComp™

Property	E_{11}	E_{22}	G_{12}	v_{12}	R_{11T}	R_{11C}	R_{22}	R_{33}	R_{12}	ρ
Unit	GPa	GPa	GPa	-	MPa	MPa	MPa	MPa	MPa	kg/m^3
Prist. CF	395	14.8	28.2	0.2	4560	-	-	-	-	1790
Rec. CF	316	14.8	28.2	0.2	4560	-	-	-	-	1790
Prist. CFRP	194	8	4.5	0.3	2320	981	49	160	67	1550
Rec. CFRP	155	8	3.6	0.3	2320	981	49	160	67	1550

2.2 Methods

We design a solution by applying and further developing the function-oriented spiral approach [36]. Specifically, we investigate the approach an engineer can take during the design phase, on the example of a hat-stiffener with skin, to fulfill on one hand the main structural function and on the other hand, to realize recycling as a function. The main structural function, given usually by a reference case, is here a structure with pristine materials. In order to realize our requirement to integrate recycling-as-a-function, we approach this problem by locally replacing pristine with recycled carbon fibers and we in parallel investigate the effect of this change to the global stiffness, depicted at the first five eigenfrequencies as well as the affected effort on typical loading conditions.

We consider recycling as a complex, societal, non-mechanical function that has to be integrated in the system, addressing the current societal challenges [38]. As with other types of functions, the integration of the functionality has to be defined and included already at the list of requirements during the design phase. Here, the recycling-as-a-function approach **aims to re-design** a hat-stiffener with skin **by increasing the percentage of recycled to pristine fibers,** which will be here stated as the recycling-index we want to achieve.

Complementary to and building on VDI 2221, the proposed design approach starts with the requirement specification, and continues in six phases of development providing as an output a draft solution. Consequently, we compare the drafted solution to the given requirements to ensure consistency between input and output and multiple iterations may occur. The six phases of a design cycle are presented in Figure 2 and form the structure of the current investigations. This cycle should assist the engineer to follow a consistent method to solve an engineering design problem to achieve multiple functionalities at the component level.

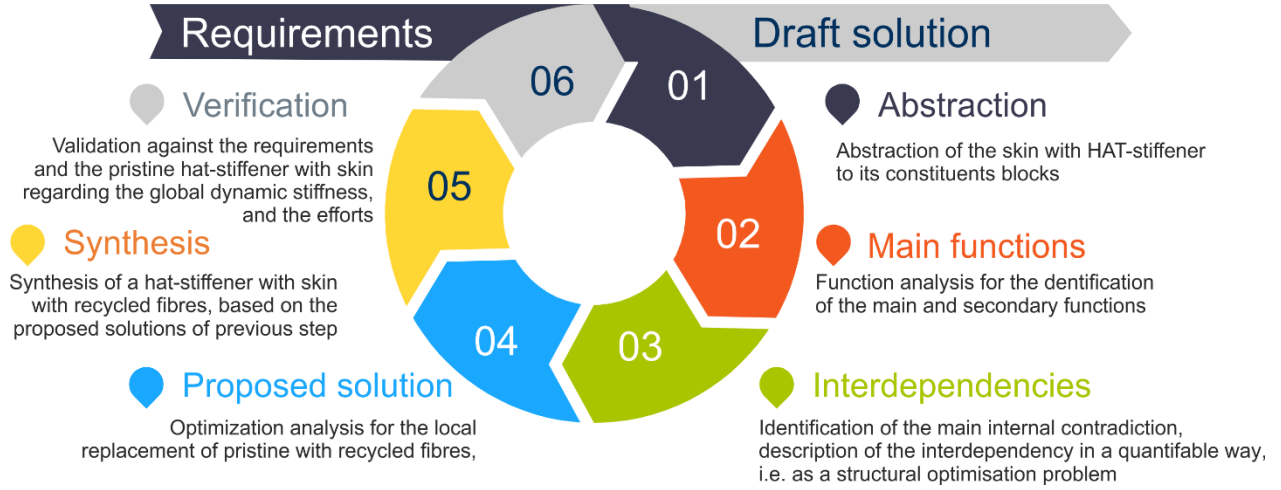

Figure 2 – Application of the spiral development approach in the case of recycling-as-a-function for a hat-stiffener with skin according to [36]

The steps are specified as follows, as shown at Figure 2:

- We define **requirements** for the actual state of the skin with hat-stiffener based on the literature [24, 25] and the target state, considering the current societal challenges.
- **We abstract** the skin with hat-stiffener to its constituent blocks in order to identify a representative topology at component and material level.
- We perform a function analysis to identify the **main functions**; structural and recycling functions inspired from the work of Koller and others [39, 40].
- We investigate the **interdependencies** and try to identify the main internal contradiction [41], and then to describe the interdependency in a quantifiable way, in this case as a structural optimization problem.
- We propose a **solution**, which are the results of an optimization analysis for the local replacement of pristine with recycled fibers.
- We perform a **synthesis** of the hat-stiffener with skin with recycled fibers, based on the

proposed solutions of previous step, taking into consideration common engineering knowledge on composites and their manufacturing possibilities.

- As the last step we **verify** against the requirements and the validation against the pristine hat-stiffener with skin regarding the global dynamic stiffness, and the efforts under typical loading conditions.

To realize the requirements, we formulate a constrained optimization problem that attempts to find an optimal spatial distribution of combination of pristine and recycled fibers; this hybrid structure with pristine and recycled fibers simultaneously fulfills the structural and recyclability functions. For solving optimization problems with such complex objectives, the use of gradient-free algorithms, such as binary-representation based genetic algorithms is investigated. The genetic algorithms simulate the objective function in a simplified way to achieve desired optimization of the given objective. The algorithms employ population of individuals encoded in a binary string format [37], which represent a possible solution to the given problem. A step-by-step implementation [30] of a binary-representation based genetic algorithm is illustrated in Figure 3:

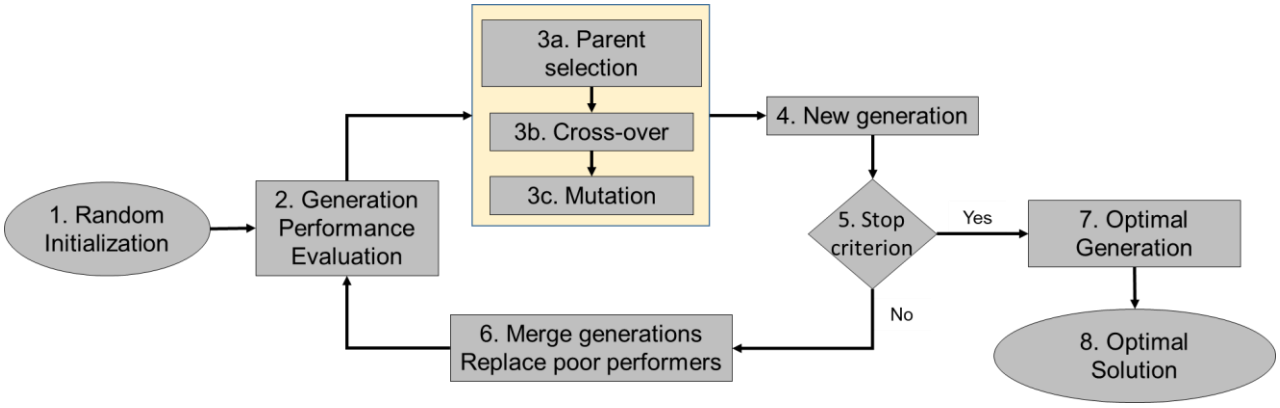

Figure 4 – Binary-representation of a typical genetic algorithm with 8 steps [30].

As shown in Figure 3, the algorithm starts with random population initialization (Step 1) by randomly generating parametrized solutions that represent wide variety of possible optimal solutions. The random generation of population is followed by performance evaluation and ranking, step 2, of the population. In step 3 binary parameters of parents are determined for crossover, through performance evaluation and ranking. The binary parameters of high-performance candidates from the population pool are then mixed together with the help of different techniques, such as single-point, two-point or randomized crossover to create new members. Newly generated members are randomly mutated to obtain population for new generation in step 4. Consecutively, the new generation is then mixed with the old generation for performance evaluation and ranking. The process is repeated until we achieve the desired objective, or the stop-criteria is met.

3. Design Phase

To explore the tradeoff between structural performance and the introduction of different mix levels of the selected recycled material, we investigate the dynamic stiffness of an aeronautical composite component presented in Section Methods and Materials.

3.1 Requirement list

We begin with the requirement specification for each functional level; in this case, we have the structural and the recycling level. The requirements set are for each level:

	Current state	Target state
Structural requirements	• Reference Stiffness	• Stiffness loss in specific range
	• No damage to the component should occur • Effort significant below damage initiation for typical loading conditions • Typical loading conditions (bending, tensile, torsion, shear) • Boundary conditions (fixed at one end) and Safety Factor (SF) of 2.0	

	• Materials for aeronautical structures • The outer geometrical dimensions of the structure should remain the same	
Recycling requirements	• No recycling requirements at current state	• Achieve a significant recycled material proportion between 10 % to 50 %, which is calculated as the percentage of recycled fibers to the total amount of fibers used • Identify relationship between stiffness loss, affected efforts to recycled material proportion

3.2 Abstraction of the system to a simpler representative geometry

It is usual not efficient to investigate a problem in its real form, due to its high complexity, or limited resources in experimental and numerical effort. In our case, we have a system of two components, the hat-stiffener and the skin. We proceed with the abstraction of each component separately. The skin can be abstracted straightforward as a composite rectangular plate. The hat-stiffener can be also abstracted as a joint system of five rectangular composite plates with length to width ratio between 3:3 and 30:8. In this sense, for the abstraction of the two components of the system, the skin and the hat-stiffener, we abstract them to a simple rectangular composite plate with symmetry boundary conditions and fixed at one end, and aspect ratio of 3:3 as shown in Figure 5.

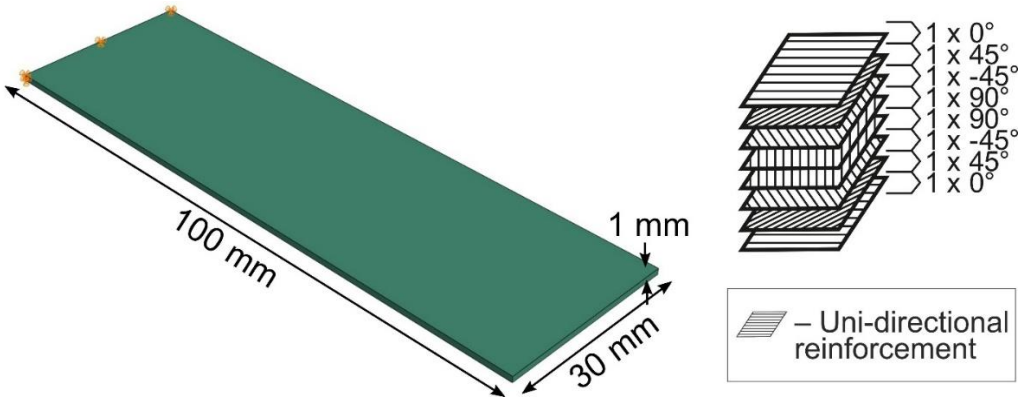

Figure 5 – Abstraction of the stiffener and the skin as a composite plate with symmetry boundary conditions and fixed at one end

Based on the structural requirement that the outer geometrical dimensions of the structure cannot be changed, the focus lies on the inner topology of the materials and their materials themselves. Hence, the internal **structure** of the materials (lay-up), which result in specific mechanical **properties**, enable a specific **functionality**. This **structure-property-function** (SPF) relation defines the internal connection of materials to the function [42]. The inclusion of the recycling function requires the adaptation of the internal structure, with the parallel goal not to significantly hinder the structural function or at least to minimize the impact on the existing structural function. For the structural functionality, we use a typical lay-up of $[0,45,-45,90]_s$ shown in Figure 5 and materials properties retrieved form the literature [8].

3.3 Identification of the Main and Secondary Functions

The main functions of the hat-stiffener with skin is its structural integrity and the new required function of recyclability. We investigate the main contradictions between these functions, with the scope to including a recycling aspect without deviating from the purpose of the original design. The **recycling function** is quantified with the introduction of the recycling index RI, which is defined as ratio of total introduced recycled material to the total used material.

$$RI = \frac{Recycled\ material}{Total\ material} \ \epsilon\ [0,1] \tag{1}$$

The **structural function** can be described as a function of the recycling index, and the distribution of the recycled fibers and their effect on the stiffness loss:

$$St_{Loss} = f(RI, fibre\ distribution) \quad (2)$$

To ensure the ability to perform under normal operational conditions, we account both for stiffness and damage initiation. Stiffness loss is expressed as the relative variation of each of the first five eigenfrequencies due to introduction of the recycled fibers, according to Eq. 3:

$$f_i = \frac{|\, ef_{i,ref} - ef_{i,rec}\,|}{ef_{i,ref}} \times 100 \quad (3)$$

Where, f_i is the relative variation in the eigenfrequency of the i[th] mode, $ef_{i,rec}$ the eigenfrequency of i[th] mode for structure with pristine and recycled fibers and $ef_{i,ref}$ the eigenfrequency of i[th] mode for the reference structure with only pristine fibers.

Finally, for damage initiation detection, we apply a simplified equivalent effort to each failure mode. According to Eq. 2, damage initiation of a ply due to tensile stress σ_{11} occurs when Eff_{11} exceeds unity, where R_{11} denotes the strength in the longitudinal direction of the reinforcement.

$$Eff_{ij} = \frac{\sigma_{ij}}{R_{ij}} \qquad i,j = \{1,2\} \quad (4)$$

Where $i,j: 1 = Direction\ longitudinal\ to\ fibre\ direction$

$i,j: 2 = Direction\ transverse\ to\ fibre\ direction$

3.4 Description of the Interdependency and the Internal Contradiction

We identify the main internal contradiction between RI and St_{Loss} and we want to describe their interdependency in a quantifiable way, such as in an analytical, simulative or semantic way. After defining recycling as a function to be considered during design, we consequently define the recycling properties and focus on the recycled-to-pristine fiber ratio (RI). As recycling carbon fibers result in up to 20% drop in tensile modulus values [9], this drop affects the material properties of the ply and the structural performance. The relation between the amount and the spatial distribution of pristine to recycled fibers with the structure's performance is quite intuitive.

For a high recycling index the structure loses some of its stiffness, and experiences a shift in eigenfrequency values. The lower tensile modulus of the recycled fibers causes them to induce lower stress for the same strain, and consequently the pristine fibers undertake higher loads. This results in higher stress in pristine fibers and to effectively higher effort in the entire structure.

Therefore, randomly increasing recycling fibers usually has contradicting effect towards performance of the structure. On the other hand, recycled fibers substituted with an optimal spatial distribution and respective orientations at adequate amount can help increase recyclability while maintaining existing structural performance. For achieving this goal, we define an optimization algorithm that minimizes the loss of structural performance, while setting a desired amount of recycled material with an optimal spatial distribution.

Setting up the optimization problem

We set up an optimization problem to quantify both the structural performance and the amount of recycled material during the optimization procedure. In this framework, the following terms are defined for the objective and constraint requirements:

1[st] objective: Eigenfrequency error

The eigenfrequency vector, $\mathcal{F}$ for the first five eigenfrequencies is compiled as:

$$\mathcal{F} = [\, f_1,\, f_2,\, f_3,\, f_4,\, f_5\,] \quad (5)$$

Where f_i is the relative error of the i[th] eigenfrequency according to eq. (3). Therefore, eigenfrequency error, $\mathcal{F}^{err}$ is given as the Euclidian norm of $\mathcal{F}$ as follows:

$$\mathcal{F}^{err} = \left|\left|\bar{\mathcal{F}}\right|\right| = \sqrt{\sum_{i=1}^{5} |\mathcal{F}_i|^2} \quad (6)$$

2nd objective: Recycling index error

The deviation between the actual and the requested recycled material proportion, $\overline{RI}$ is defined as:

$$\overline{RI} = \frac{RI^{target} - RI}{RI^{target}} \times 100 \quad (7)$$

Where, RI^{target} represents the requested recycled material proportion and is defined as:

$$RI^{target} = \frac{Target\ Recycled\ material}{Total\ material} \epsilon\ [0,1] \quad (8)$$

Within each generation, RI can potentially exceed the optimization goal. However, from the engineer's point of view, if the recycled material in the structure is more than targeted, it should not be interpreted as error and penalized. With heuristic modification, the recycling index error, Rec^{err} is defined as:

$$Rec^{err} = \max\ \{\ \overline{RI}\ , 0\ \} \quad (9)$$

Structural constraint: Effort penalty

Assuming a safety factor of 2.0 [43], the maximum allowed effort in a structure should be maintained less than or equal to 0.5. For correctly penalizing the performance of structures whose effort is above 0.5, we define the Effort penalty based on the well-known sigmoid function as:

$$Eff^p{}_{ij} = \frac{100}{1+e^{(-1000\times(Eff_{ij}-0.49))}} \qquad i,j = \{1,2\} \quad (10)$$

According to eq.10 we introduce three penalizing terms:

Longitudinal effort penalty ($Eff^p{}_{11}$) is given as: $Eff^p{}_{11}$ = max $\{Eff^p{}_{11+}, Eff^p{}_{11-}\}$ (11)

Transverse effort penalty ($Eff^p{}_{22}$) is given as: $Eff^p{}_{22}$ = max $\{Eff^p{}_{22+}, Eff^p{}_{22-}\}$ (12)

Shear effort penalty ($Eff^p{}_{12}$) is given as: $Eff^p{}_{12}$ = max $\{Eff^p{}_{12+}, Eff^p{}_{12-}\}$ (13)

where,

$Eff^p{}_{11+}$ is the effort penalty for positive stress in longitudinal direction

$Eff^p{}_{11-}$ is the effort penalty for negative stress in longitudinal direction

$Eff^p{}_{22+}$ is the effort penalty for positive stress in transverse direction

$Eff^p{}_{22-}$ is the effort penalty for negative stress in transverse direction

$Eff^p{}_{12+}$ is effort penalty for positive stress in shear

$Eff^p{}_{12-}$ is the effort penalty for negative stress in shear

The error functional (ϕ) is given as:

$$\phi = [\ \bar{\mathcal{F}}^{err}, Rec^{err}, Eff^p{}_{11}, Eff^p{}_{22}, Eff^p{}_{12}] \quad (14)$$

Through Euclidian norm of error functional we introduce the term "Structural Performance Loss", where we convert the multi-objective error minimization problem into a single objective error minimization.

$$\textbf{Structural Performance Loss } SP_{loss}, = ||\ \widetilde{\phi}\ || = \sqrt{\sum_{i=1}^{5} |\ \boldsymbol{\phi_i}|^2} \quad (15)$$

The quantity Structural Performance Loss (SP_{loss}) is a function of the resulting stiffness of the plies with pristine and recycled fibers, which depends on the spatial distribution and amount of the recycled fibers in the structure.

Structural optimization problem

Finding the optimum topology and the spatial distribution of best suiting reinforcement for complex loading conditions is a structural optimization problem that has to be addressed during the design phase [25]. To address the search space of thousands unique reinforcement configurations, binary-representation-based genetic algorithm [44] is used to identify the optimal configurations in terms of performance and computational time. The algorithms is coupled using MATLAB as the optimization platform with a finite element solver in ABAQUS Software packet to perform a closed-loop structural topology optimization [45].

The optimization problem for a composite structure with recycled fibers is defined as:

$$\begin{cases} \text{Minimize } \mathbf{Structural\ Performance\ Loss}\ \ SP_{loss}\left(\tilde{\chi}(\zeta)\right) \\ \text{Subject to, } \zeta_{min} < RI^{target} < \zeta_{max} \end{cases} \tag{16}$$

With, $\zeta_{min} < RI^{target} < \zeta_{max}$, where $\tilde{\chi}$ is the parametrized finite element model of the structure with recycled plies; ζ the solution search space for recycled material index; ζ_{min} being the minimum allowed recycled material index and ζ_{max} the maximum allowed recycled material index.

The structural optimization problem is formulated using the norm of the eigenfrequency error and recycling index error as objective function which is to be minimized. The constraints of this optimization problem are the stress-efforts in longitudinal, transverse, and shear directions. The design variable is the spatial distribution (amount and spatial distribution) of recycled filaments, whereas the thickness of the ply is assumed to be constant. For finding optimal spatial distribution and the corresponding parametrized model to minimize the structural performance loss, we use a binary-representation-based genetic algorithm.

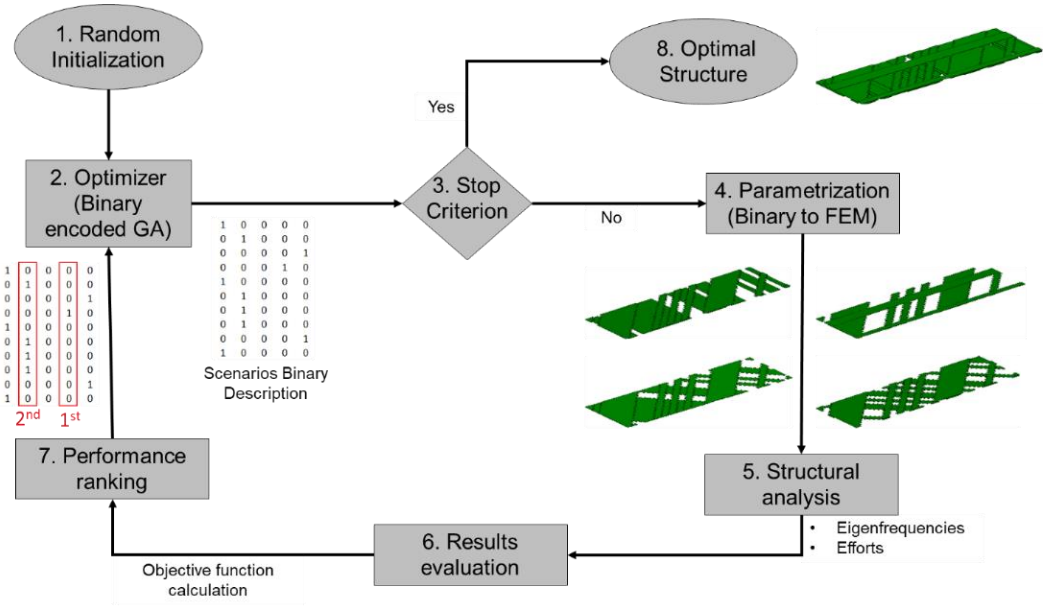

Figure 6 - Optimization flowchart for the abstracted plate with 8 steps beginning from the initialization to the suggestion of an optimal structure with pristine and recycled fibers

We implement the previously described genetic algorithm for solving the structural optimization problem of the plate. As illustrated in Figure 6, the algorithm starts by generating randomly initialized, binary-represented population (step 1). This binary population is then passed to parametrization algorithm, which, in step 4, transforms the binary into a unique ABAQUS input file. The set of input files is then given to ABAQUS for structural analysis to obtain eigenfrequencies and efforts, step 5. The results are then evaluated (step 6) to calculate the objective function '**Structural performance loss**' for every ABAQUS input file. These evaluations are then passed to the parametrization algorithm (step 7) to record and rank the performance of every binary member. The ranking of these binary members serves as a feedback to the optimizer. Based on this feedback, the optimizer, in step 2, generates new binary members and the process is repeated until convergence is reached,

or the stop-criteria defined in step 3 are met. At the end of the procedure, the optimizer yields the optimal structure in step 8.

3.5 Suggested Solution using a Simulation Model

After we have identified the main internal contradiction and described the interdependency as a structural optimization problem, we generate a finite element model of the abstracted plate to be used for the solution of the optimization problem.

The finite element model of a composite plate with the previously presented lay-up is developed making use of the general purpose commercial software ABAQUS. Based on a sensitivity study on mesh size, type, and section points' number, the SC8R three-dimensional continuum shell element is preferred. SC8R is an 8-node hexahedron general-purpose element accounting for membrane strains. A relatively dense mesh with a total number of 12,852 nodes and 10,720 elements is used. For the boundary conditions of the model, the degrees of freedom located at the one short edge of the plate are constrained in order to account for the applied boundary conditions. Each layer is modelled with one element in the thickness direction. A numerical modal analysis is performed to extract the first five eigenfrequencies, Figure 7. The plate shows normal dynamic behavior with typical mode bending, torsion and mixed shapes. Subsequently, a quasi-static static analysis is performed under four different loading conditions of axial tension, bending, torsion and shear. Loads are applied on a reference point (RP) tied to the free face along the longitudinal direction of the plate, as shown in Figure 7.

For the development of the parametric simulation, the finite element model is combined with in-house developed MATLAB scripts for the generation of multiple models with different material configurations among the plies. The change of pristine to recycled fibers is modelled as the change of the material properties at selected elements along the layup orientation. The selected dense mesh provides adequate resolution for realistic distinction between the two types of fibers along each ply direction. The variation in eigenfrequencies and the efforts due to the change at the material of the plate constitute the input for the optimization function.

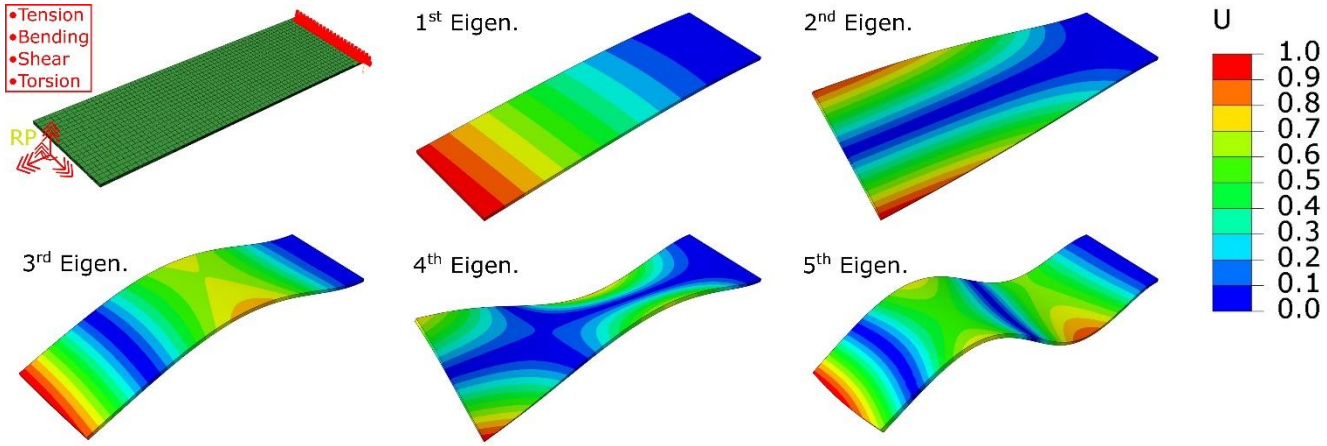

Figure 7 – Finite element model with loading and boundary conditions of the abstracted plate and estimated first five mode shapes

Regarding the whole range of the examined scenarios, presented in Table 2, an increasing recycling index from 10 % to 50 %, has a relative minimum impact on the global dynamic stiffness depicted at the first five eigenfrequencies for the abstracted optimized composite plate. Specifically, we observe a relative shift of the torsional eigenmode of 4.3 %, due to the relative high (54%) substitute of pristine with recycled fibers at the 45° direction and a relative shift of all bending eigenmodes of 2.3 %.

Table 2 - Effect of increasing recycled material to the first 5 eigenfrequencies for the abstracted

optimized composite plate

Eigenfreq.	*EF1*		*EF2*		*EF3*		*EF4*		*EF5*	
Mode shape	1st bending		1st torsion		2nd bending		1st mixed		3rd bending	
Unit	Hz	%	Hz	%	Hz	%	Hz	%	Hz	%
Ref. RI=0%	4.70	0.00	21.43	0.00	29.19	0.00	70.91	0.00	81.63	0.00
RI = 10%	4.69	-0.05	21.35	-0.37	29.17	-0.07	70.66	-0.36	81.54	-0.11
RI = 20%	4.67	-0.51	21.30	-0.59	29.04	-0.53	70.34	-0.81	81.18	-0.55
RI = 30%	4.63	-1.48	21.09	-1.60	28.75	-1.51	69.92	-1.40	80.48	-1.41
RI = 40%	4.66	-0.79	20.87	-2.61	28.96	-0.80	69.17	-2.45	80.93	-0.86
RI = 50%	4.59	-2.32	20.50	-4.32	28.53	-2.28	68.20	-3.83	79.75	-2.31

The preciously described contradiction between the recycling index and the structural performance is also depicted in Figure 8. Specifically, Figure 8 (a) illustrates a direct dependency of eigenfrequency reduction with respect to recycling index. Whereas, Figure 8b illustrates a pattern of increase in effort for increasing recycling index. This approach allow us to evaluate the proposed solutions and select the most promising to be able to realize both the structural as well as the recycling function.

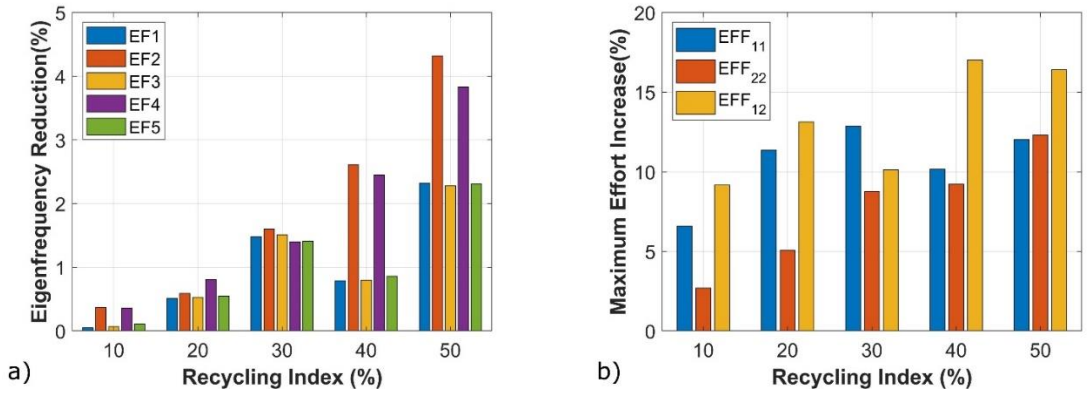

Figure 8 - Effect of increasing recycled index to a) the first 5 eigenfrequencies and b) the maximum effort per load case for the abstracted composite plate

Considering that RI = 30 % provides a good trade-off between recycling and structural functions, Figure 9 illustrates a detailed optimization history for further investigation. After running for 100 generations, the evolution of distribution of recycled material per ply of the best member is extracted and illustrated in Figure 9a. The position of the recycled fibers and the affected efforts are also stored for further analysis and illustration purposes. The structural performance loss is shown in Figure 9b for each generation converging to approximately 3.5 %.

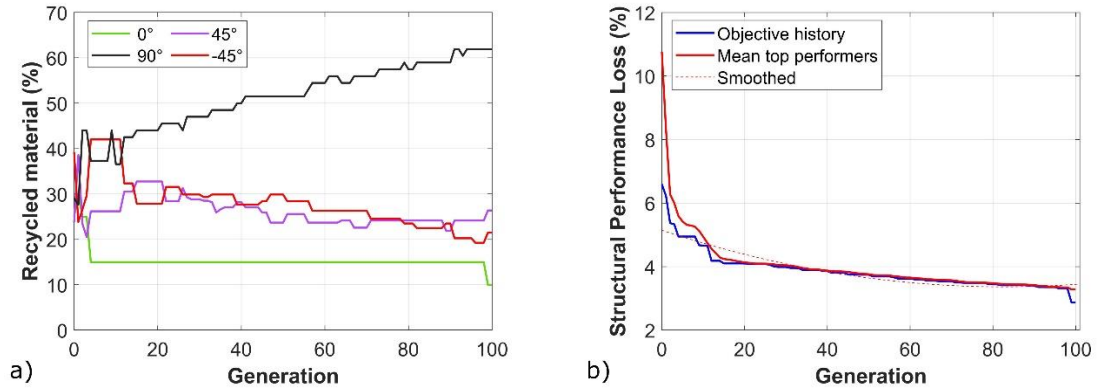

Figure 9: Results of the a) optimization process from the plate for all investigated layers and b) convergence chart

For the same RI of 30 %, Table 3 summarizes a compilation of the applied loading conditions and the corresponding efforts. It is worth noting, that the highest effort increase (ΔEff_{11} = 12.85%) is observed for the tensile loading case, where the reference effort did not exceed 0.14. This implies that the optimizer identifies the wide possible margin of increase for the non-critical loading conditions. On the

other hand, for the reference configuration the efforts that were close to the maximum allowed limit of 0.5 were diminishingly affected, meaning that pristine fibers contributing the most to the critical loading conditions were kept mostly unchanged. A full overview of efforts for RIs in the range of 10% to 50% is provided in the Appendix.

Table 3 – Effect on efforts for the optimized model for a recycling index **RI of 30%**

Load case	**Stress**	EFF_{11}	EFF_{22}	EFF_{12}	EFF_{11}	EFF_{22}	EFF_{12}	ΔEFF_{11}	ΔEFF_{22}	ΔEFF_{12}
		Reference RI=0%			**RI= 30%**					
Unit	-	-	-	-	-	-	-	%	%	%
Bending	σ_{ij}^{+}	0.19	0.18	0.17	0.19	0.18	0.18	2.53	3.88	4.05
	σ_{ij}^{-}	0.45	0.06	0.17	0.47	0.05	0.17	3.31	4.64	2.93
Tensile	σ_{ij}^{+}	0.22	0.45	0.27	0.23	0.47	0.28	7.58	6.38	8.77
	σ_{ij}^{-}	0.14	0.03	0.27	0.15	0.03	0.28	12.85	10.13	8.77
Torsion	σ_{ij}^{+}	0.19	0.21	0.21	0.19	0.22	0.22	2.90	6.94	4.68
	σ_{ij}^{-}	0.46	0.06	0.21	0.47	0.06	0.22	3.37	7.04	5.73
Shear	σ_{ij}^{+}	0.20	0.36	0.24	0.20	0.36	0.24	2.66	1.53	2.69
	σ_{ij}^{-}	0.46	0.12	0.24	0.46	0.12	0.24	1.38	-0.10	2.69

3.6 Synthesis of a hat-stiffener with skin with recycled fibers

After successfully demonstrating promising results for the abstracted version of the studied problem, the developed approach is applied on the hat-stiffener configuration. At the synthesis step, we try to fuse the information gained from the abstraction of the problem, with the current engineering and expert knowledge. The previously described modeling assumptions and procedure for the simulation of the composite plate have been also adapted for the hat-stiffener. Based on the conducted mesh convergence the examined part was discretized with approximately 60,000 elements, as shown in Figure 10. The observed increase on elements is attributed to the additional plies and complexity of the geometry.

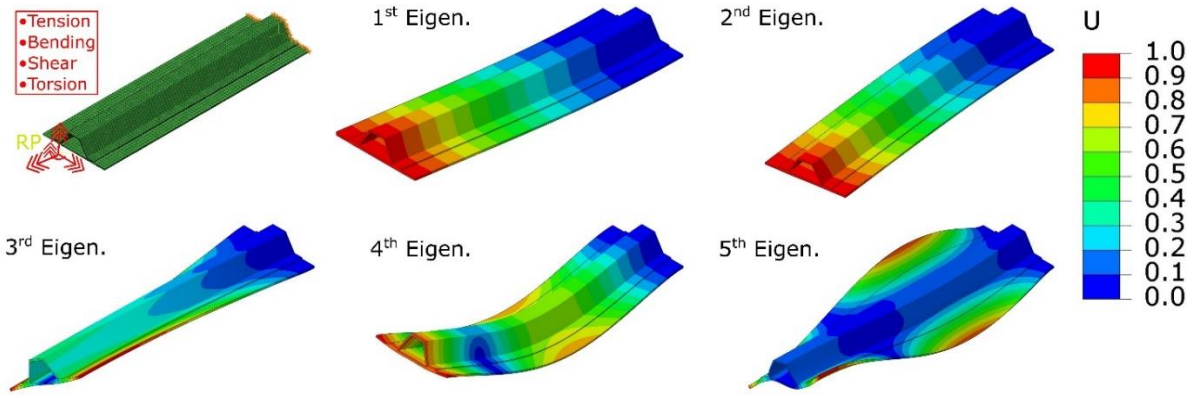

Figure 10 – Finite element model with loading and boundary conditions of the stiffener-hat with skin and estimated first five mode shapes of same type as in the case of the abstracted plate

Figure 10 depicts the first five mode shapes of the examined configuration. A comparison with the abstracted plate and the resulting mode shapes, shown in Figure 7, reveals that for both geometries, similar mode shapes exist, mainly bending and torsional related shapes. This observation strengthens the abstraction validity by highlighting the similar response of the both structures. The data we retrieve during the optimization process is the layup with pristine and recycled fibers, their orientation, the respective efforts and eigenfrequencies.

Table 4 summarizes the effects of the recycled fibers on the stiffness of the studied component. It is worth noting that for the critical first mode (EF1), the natural frequency drop does not exceed 1% even at RI=50%. The eigenfrequency reduction gradually intensifies up to 2.08% for the torsional

mode (EF3) and for maximum RI.

Table 4 - Effect of increasing recycled material to the absolute and relative change of the first five eigenfrequencies for the hat-stiffener with skin

Eigenfreq.	*EF1*		*EF2*		*EF3*		*EF4*		*EF5*	
Mode shape	1st bending		2nd bending		1st torsion		3rd bending		1st mixed	
Unit	Hz	%	Hz	%	Hz	%	Hz	%	Hz	%
Ref. RI=0%	2.64	0.00	8.34	0.00	12.07	0.00	14.59	0.00	31.14	0.00
RI = 10%	2.64	0.00	8.34	0.00	12.06	-0.07	14.58	-0.04	31.09	-0.17
RI = 20%	2.63	-0.11	8.33	-0.06	12.04	-0.26	14.56	-0.20	31.01	-0.41
RI = 30%	2.63	-0.28	8.32	-0.23	11.96	-0.90	14.53	-0.40	30.88	-0.84
RI = 40%	2.62	-0.82	8.29	-0.60	11.91	-1.31	14.40	-1.30	30.52	-2.00
RI = 50%	2.61	-0.96	8.28	-0.65	11.82	-2.08	14.38	-1.45	30.49	-2.07

To obtain a better insight into the derived optimal configurations, the proposed solution for RI=30% is described through Figure 11 and Figure 12. In detail, Figure 11 presents the evolution of top performing distribution of recycled material within each ply direction per generation. The optimal solution which is also visualized in Figure 12 constitutes of 45% recycled material along the 90° ply and an equally sized stripe of recycled material for 45° and -45° plies. The importance of the fibers strength along the longitudinal direction is illustrated by the absence of extensive recycled material use in the 0° ply.

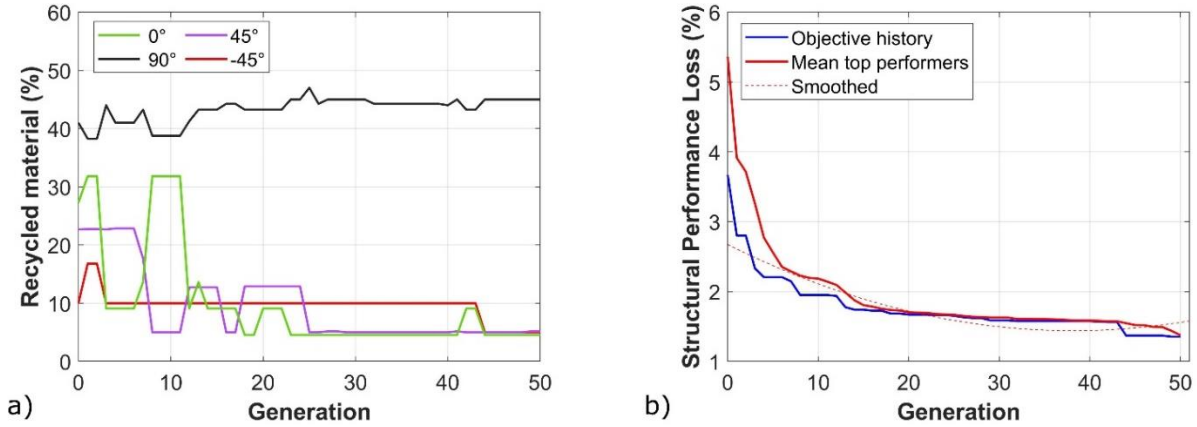

Figure 11 - Results of the optimization process from the hat-stiffener with skin a) for all investigated layers and b) convergence chart for RI = 30 %.

The knowledge we add during the synthesis step is to enabling secondary functions, for example the ability to manufacture the proposed component. Since we have already accounted for plies symmetry along the stacking direction, avoiding problems during curing of the component and layup-dependent permanent deformations, we modify the proposed solution to acquire symmetry along the YZ plane (Figure 1). This implies that symmetry of the 0°, 45° and -45° plies along the longitudinal direction of the hat is introduced, Figure 12.

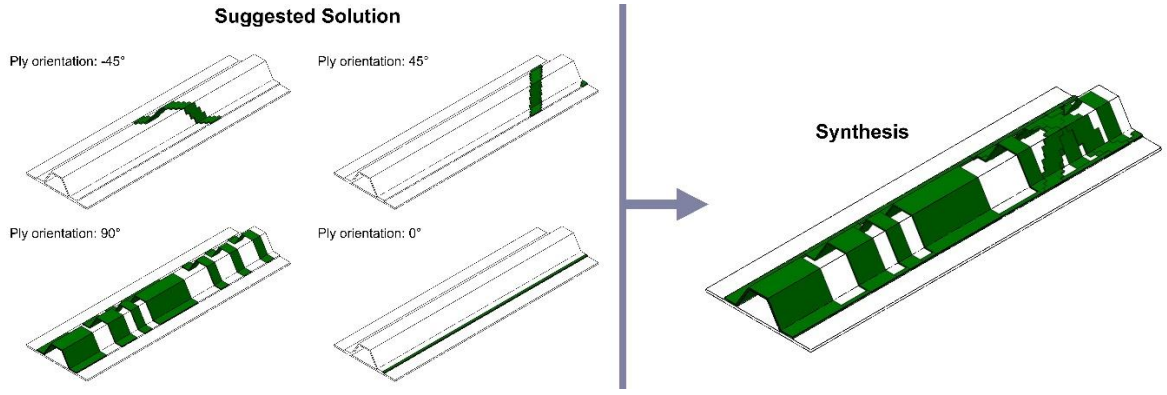

Figure 12 - Results of the optimization process from the hat-stiffener for the optimized layers; highlighted with green are the proposed substitution of pristine with recycled fibers

3.7 Validation against the requirements and the reference structure

The last step of the design approach is the validation against the requirements and the reference structure. Therefore, we virtually validate the results from the structural optimization, especially we investigate whether the proposed solution agrees with the requirement list, Table 5, similar to (46). In case of a discrepancy, a new iteration should then occur.

Table 5 - Main results from the validation step to ensure both structural and recycling functionalities for the hat-stiffener with skin

	Target state
Structural requirements	• Low relative eigenfrequency value reduction in the range of 2 % - 5 %
	• Selected materials suitable for aeronautical structures if they pass a respective certification procedure; still open to be addressed in the future • The outer geometrical dimensions of the structure have remained the same • No significantly effort increase was observed that could lead to damage initiation and propagation to the component • Effort significant below damage initiation for typical loading conditions (bending, tensile, torsion, shear), effort in not-critical areas increased with recycled fibers
Recycling requirements	• Achieved a significant recycled material proportion for relative low change of global dynamic stiffness, and effort. • Identified a non-linear relationship between the stiffness loss, and the affected efforts to the increasing recycled material proportion.

For an increase of recycled material in the hat-stiffener, we observe approximate relative decrease of 2 % in eigenfrequency values, whereas relative increase of 12 % in efforts for non-critical loading scenarios. As suggested by the optimizer, it would be possible to include up to 50 % of recycled material in plies with low efforts and to maintain a low relative eigenfrequency loss of 2 %.

We conclude that the results comply with the original requirements. It is important here to note that these validated solution holds true for the given loading conditions and a change at the list of requirements should prompt for a new iteration. In general, a change at the requirement list affects one or more steps of the development approach. For example, changes at the geometry of the component may lead to a new abstraction of the geometry. The manufacturing of such a component should be possible using various textile manufacturing methods, e.g. the tailored-fiber placement method. Mainly the challenge originates from the quality and quantity of the current recycled fibers. Especially, the problems of undulation and length of recycled fibers, their high scatter of mechanical properties should be further addressed at the near future.

4. Summary & Outlook

We propose a design approach to include recyclability as a function for a typical aeronautical component. We work on two main levels. The first level is the theoretical part of developing a design approach, which assists a design engineer to include new functionalities at complex structures. With this approach, it is possible to work with identifying main and secondary functions, describing their interdependencies, identifying the internal contradictions and trying to design by solving the internal contradictions. The second level is to depict this theoretical framework to a typical aeronautical structure, on the example of integrating a new functionality, in our case to include recycling material to the structure. To achieve a design solution, we interpret the interdependencies as a structural optimization problem, we select a gradient-free genetic algorithm to identify the relations between structural and recycling functions and provide first solutions to the described contradiction.

The **preliminary results** demonstrate that for specific loading conditions, we can achieve an increased recycled-to-pristine fibers ratio given a low stiffness loss by introducing local adaptations to the **fiber reinforcement**. The **key findings** consist of a better understanding of the steps that a design engineer has to consider, when trying to include recyclability as a function to a representative structural component by replacing pristine with recycled fibers. Furthermore, results from the

structural optimization will provide valuable hints on the possibility of using future continuous recycled fibers at complex loaded composite structures. Further investigations in this direction should include both the theoretical design framework, as well as the identification of suitable applications for introducing new functionalities, such as the recyclability.

5. Contact Author Email Address

Mailto: Angelos Filippatos angelos.filippatos@tu-dresden.de

6. Copyright Statement

References

[1] Alderliesten R. On the development of hybrid material concepts for aircraft structures. *Recent Patents on Engineering* 2009 **3** 25–38.
[2] F. Kocian, P. Ebel, Björn Drees, K. Schulze, J. Hausmann & H. Voggenreiter. Hybrid structures in aero engines. *undefined* 2015.
[3] Reuter MA. Limits of design for recycling and "sustainability": a review. *Waste and Biomass Valorization* 2011 **2** 183–208.
[4] Heibeck M, Rudolph M, Modler N, Reuter M & Filippatos A. Characterizing material liberation of multi-material lightweight structures from shredding experiments and finite element simulations. *Minerals Engineering* 2021 **172** 107142.
[5] Markatos DN, Katsiropoulos CV, Tserpes KI & Pantelakis SG. A holistic End-of-Life (EoL) Index for the quantitative impact assessment of CFRP waste recycling techniques. *Manufacturing Review* 2021 **8** 18.
[6] Asmatulu E, Overcash M & Twomey J. Recycling of aircraft: state of the art in 2011. *Journal of Industrial Engineering* 2013 **2013** 1–8.
[7] Markatos DN & Pantelakis SG. Assessment of the impact of material selection on aviation sustainability, from a circular economy perspective. *Aerospace* 2022 **9** 52.
[8] Yang Y, Boom R, Irion B, van Heerden D-J, Kuiper P & Wit H de. Recycling of composite materials. *Chemical Engineering and Processing: Process Intensification* 2012 **51** 53–68.
[9] Yang J, Liu J, Liu W, Wang J & Tang T. Recycling of carbon fibre-reinforced epoxy resin composites under various oxygen concentrations in nitrogen–oxygen atmosphere. *Journal of Analytical and Applied Pyrolysis* 2015 **112** 253-261.
[10] Hao S, He L, Liu J, Liu Y, Rudd C & Liu X. Recovery of carbon fibre from waste prepreg via microwave pyrolysis. *Polymers* 2021 **13**.
[11] Clean Aviation. Born again: Obsolete composites find a second life with RESET. (accessed 18 May 2022).
[12] Hüther JJ. *The impact of recycling on the fibre and the composite properties of carbon fibre reinforced plastics*, Dissertation: KIT Scientific Publishing, 2019.
[13] Bachmann J, Wiedemann M & Wierach P. Flexural mechanical properties of hybrid epoxy composites reinforced with nonwoven made of flax fibres and recycled carbon fibres. *Aerospace* 2018 **5** 107.
[14] Wong K, Rudd C, Pickering S & Liu X. Composites recycling solutions for the aviation industry. *Science China Technological Sciences* 2017 **60** 1291–1300.
[15] Wang B, Ma S, Yan S & Zhu J. Readily recyclable carbon fiber reinforced composites based on degradable thermosets: a review. *Green Chemistry* 2019 **21** 5781–5796.
[16] Pimenta S & Pinho ST. The effect of recycling on the mechanical response of carbon fibres and their composites. *Composite Structures* 2012 **94** 3669–3684.
[17] Q. Zhao, Jianjun Jiang, Chuanbing Li & Yujun Li. Efficient recycling of carbon fibers from amine-cured CFRP composites under facile condition. *undefined* 2020.
[18] Simon J, Hamila N, Binetruy C, Comas-Cardona S & Masseteau B. Design and numerical modelling strategy to form Tailored Fibre Placement preforms: Application to the tetrahedral part with orthotropic final configuration. *Composites Part A: Applied Science and Manufacturing* 2022 **158** 106952.
[19] Carey JP, Melenka GW, Hunt A, Cheung B, Ivey M & Ayranci C. Braided composites in aerospace engineering 175–212.
[20] Peters ST, Humphrey WD & Foral RF. *Filament winding - Composite structure fabrication*: Covina, CA; Society for the Advancement of Material and Process Engineering, 1991.
[21] *Guideline VDI 2221: Methodik zum Entwickeln und Konstruieren technischer Systeme und Produkte*, Düsseldorf,

VDI-Verlag, 1993.
[22] Vitali R, Park O, Haftka RT, Sankar BV & Rose CA. Structural optimization of a hat-stiffened panel using response surfaces. *Journal of Aircraft* 2002 **39** 158–166.
[23] Jin BC, Li X, Mier R, Pun A, Joshi S & Nutt S. Parametric modeling, higher order FEA and experimental investigation of hat-stiffened composite panels. *Composite Structures* 2015 **128** 207–220.
[24] Barkanov E, Ozoliņš O, Eglītis E, Almeida F, Bowering MC & Watson G. Optimal design of composite lateral wing upper covers. Part I: Linear buckling analysis. *Aerospace Science and Technology* 2014 **38** 1–8.
[25] Barkanov E, Eglītis E, Almeida F, Bowering MC & Watson G. Optimal design of composite lateral wing upper covers. Part II: Nonlinear buckling analysis. *Aerospace Science and Technology* 2016 **51** 87–95.
[26] Windarto, Indratno SW, Nuraini N & Soewono E. A comparison of binary and continuous genetic algorithm in parameter estimation of a logistic growth model, pp 139–142: AIP Publishing LLC, 2014.
[27] Holland JH. Genetic algorithms and adaptation. In *Adaptive Control of Ill-Defined Systems*, pp 317–333. Eds OG Selfridge, EL Rissland & MA Arbib. Boston, MA: Springer, 1984.
[28] Goldberg DE, Korb B & Deb K. Messy genetic algorithms: motivation, analysis, and first results. *Complex Systems* 1989 **3** 493–530.
[29] Hu X-B & Di Paolo E. Binary-representation-based genetic algorithm for aircraft arrival sequencing and scheduling. *IEEE Transactions on Intelligent Transportation Systems* 2008 **9** 301–310.
[30] Haupt RL & Haupt SE. *Practical genetic algorithms*, edn 2. Hoboken N.J.: John Wiley, 2004.
[31] Zingg DW, Nemec M & Pulliam TH. A comparative evaluation of genetic and gradient-based algorithms applied to aerodynamic optimization. *European Journal of Computational Mechanics* 2008 **17** 103–126.
[32] Paluch B, Grédiac M & Faye A. Combining a finite element programme and a genetic algorithm to optimize composite structures with variable thickness. *Composite Structures* 2008 **83** 284–294.
[33] Yan G & Zhou L. Impact load identification of composite structure using genetic algorithms. *Journal of Sound and Vibration* 2009 **319** 869–884.
[34] Lin C-C & Lee Y-J. Stacking sequence optimization of laminated composite structures using genetic algorithm with local improvement. *Composite Structures* 2004 **63** 339–345.
[35] Swanson GD, Gurdal Z & Starnes JH. Structural efficiency study of graphite-epoxy aircraft rib structures. *Journal of Aircraft* 1990 **27** 1011–1020.
[36] Modler N, Winkler A, Filippatos A, Weck D & Dannemann M. Function-integrative lightweight engineering – design methods and applications. *Chemie Ingenieur Technik* 2020 **92** 949–959.
[37] Sarker R. *Evolutionary optimization*. Boston, MA: Kluwer Academic Publishers, 2003.
[38] Dumée LF. Circular materials and circular design-review on challenges towards sustainable manufacturing and recycling. *Circular economy and sustainability* 2022 **2** 9–23.
[39] Koller R. *Konstruktionslehre für den Maschinenbau: Grundlagen zur Neu- und Weiterentwicklung technischer Produkte mit Beispielen*, edn 3. Berlin, Heidelberg, s.l.: Springer Berlin Heidelberg, 1994.
[40] *A methodical approach for designing innovative products based on computer aided functional modelling*, 2013.
[41] Cavallucci D. *TRIZ – The theory of inventive problem solving*. Cham: Springer International Publishing, 2017.
[42] Chen C, Kuang Y, Zhu S, Burgert I, Keplinger T, Gong A, Li T, Berglund L, Eichhorn SJ & Hu L. Structure–property–function relationships of natural and engineered wood. *Nature Reviews Materials* 2020 **5** 642–666.
[43] Zipay JJ, Modlin CT & Larsen CE. The ultimate factor of safety for aircraft and spacecraft - its history, applications and misconceptions. In *57th AIAA/ASCE/AHS/ASC Structures, Structural Dynamics, and Materials Conference*. Reston, Virginia: American Institute of Aeronautics and Astronautics, 01042016.
[44] Muc A & Gurba W. Genetic algorithms and finite element analysis in optimization of composite structures. *Composite Structures* 2001 **54** 275–281.
[45] Sun XF, Yang J, Xie YM, Huang X & Zuo ZH. Topology optimization of composite structure using bi-directional evolutionary structural optimization method. *Procedia Engineering* 2011 **14** 2980–2985.
[46] Smolnicki M & Stabla P. Finite element method analysis of fibre-metal laminates considering different approaches to material model. *SN Applied Sciences* 2019 **1**.

Appendix

Results for the **abstracted plate** at three different efforts for four loading cases of five tests cases with an increasing recycling index from 10 % to 50 %

Case 1: Targeted recycled fibers index: RI= 10%

Load case	Stress	Eff_{11}	Eff_{22}	Eff_{12}	Eff_{11}	Eff_{22}	Eff_{12}	ΔEff_{11}	ΔEff_{22}	ΔEff_{12}
		Reference RI=0%			RI= 10%					
Unit	-	-	-	-	-	-	-	%	%	%
Bending	σ_{ij}^{+}	0.19	0.18	0.17	0.19	0.18	0.17	0.16	0.19	0.34
	σ_{ij}^{-}	0.45	0.06	0.17	0.46	0.06	0.17	0.13	0.04	0.09
Tensile	σ_{ij}^{+}	0.22	0.45	0.27	0.23	0.46	0.27	2.52	1.04	1.57
	σ_{ij}^{-}	0.14	0.03	0.27	0.15	0.04	0.27	6.58	9.17	2.47

Torsion	σ_{ij}^{+}	0.19	0.21	0.21	0.20	0.21	0.22	1.47	1.25	0.91
	σ_{ij}^{-}	0.46	0.06	0.21	0.46	0.07	0.22	0.76	3.76	1.82
Shear	σ_{ij}^{+}	0.20	0.36	0.24	0.20	0.36	0.24	2.16	0.68	2.69
	σ_{ij}^{-}	0.46	0.12	0.24	0.46	0.12	0.24	1.56	-0.31	2.69

Case 2: Targeted recycled fibers index: RI= 20%

Load case	**Stress**	***Eff*$_{11}$**	***Eff*$_{22}$**	***Eff*$_{12}$**	***Eff*$_{11}$**	***Eff*$_{22}$**	***Eff*$_{12}$**	**Δ*Eff*$_{11}$**	**Δ*Eff*$_{22}$**	**Δ*Eff*$_{12}$**
		Reference RI=0%			**RI= 20%**					
Unit	-	-	-	-	-	-	-	%	%	%
Bending	σ_{ij}^{+}	0.19	0.18	0.17	0.20	0.19	0.17	1.73	3.08	0.00
	σ_{ij}^{-}	0.45	0.06	0.17	0.46	0.06	0.18	0.31	0.35	3.10
Tensile	σ_{ij}^{+}	0.22	0.45	0.27	0.23	0.47	0.28	3.17	4.08	5.06
	σ_{ij}^{-}	0.14	0.03	0.27	0.15	0.04	0.28	11.36	13.13	5.06
Torsion	σ_{ij}^{+}	0.19	0.21	0.21	0.20	0.23	0.22	2.41	6.76	2.73
	σ_{ij}^{-}	0.46	0.06	0.21	0.47	0.07	0.22	2.59	4.73	4.12
Shear	σ_{ij}^{+}	0.20	0.36	0.24	0.20	0.36	0.24	2.02	1.19	2.51
	σ_{ij}^{-}	0.46	0.12	0.24	0.46	0.12	0.24	1.36	0.98	2.51

Case 3: Targeted recycled fibers index: RI= 30%

Load case	**Stress**	***Eff*$_{11}$**	***Eff*$_{22}$**	***Eff*$_{12}$**	***Eff*$_{11}$**	***Eff*$_{22}$**	***Eff*$_{12}$**	**Δ*Eff*$_{11}$**	**Δ*Eff*$_{22}$**	**Δ*Eff*$_{12}$**
		Reference RI=0%			**RI= 30%**					
Unit	-	-	-	-	-	-	-	%	%	%
Bending	σ_{ij}^{+}	0.19	0.18	0.17	0.20	0.19	0.18	2.53	3.88	4.05
	σ_{ij}^{-}	0.45	0.06	0.17	0.47	0.06	0.18	3.32	4.64	2.93
Tensile	σ_{ij}^{+}	0.22	0.45	0.27	0.24	0.48	0.29	7.59	6.39	8.77
	σ_{ij}^{-}	0.14	0.03	0.27	0.15	0.04	0.29	12.86	10.13	8.77
Torsion	σ_{ij}^{+}	0.19	0.21	0.21	0.20	0.23	0.22	2.91	6.95	4.68
	σ_{ij}^{-}	0.46	0.06	0.21	0.47	0.07	0.23	3.37	7.05	5.73
Shear	σ_{ij}^{+}	0.20	0.36	0.24	0.20	0.36	0.24	2.66	1.53	2.69
	σ_{ij}^{-}	0.46	0.12	0.24	0.46	0.12	0.24	1.39	-0.10	2.69

Case 4: Targeted recycled fibers index: RI= 40%

Load case	**Stress**	***Eff*$_{11}$**	***Eff*$_{22}$**	***Eff*$_{12}$**	***Eff*$_{11}$**	***Eff*$_{22}$**	***Eff*$_{12}$**	**Δ*Eff*$_{11}$**	**Δ*Eff*$_{22}$**	**Δ*Eff*$_{12}$**
		Reference RI=0%			**RI= 40%**					
Unit	-	-	-	-	-	-	-	%	%	%
Bending	σ_{ij}^{+}	0.19	0.18	0.17	0.20	0.19	0.17	2.08	3.93	-1.21
	σ_{ij}^{-}	0.45	0.06	0.17	0.46	0.06	0.18	0.92	-0.50	1.64
Tensile	σ_{ij}^{+}	0.22	0.45	0.27	0.23	0.47	0.28	5.18	4.62	6.24
	σ_{ij}^{-}	0.14	0.03	0.27	0.15	0.04	0.28	10.16	17.02	4.89
Torsion	σ_{ij}^{+}	0.19	0.21	0.21	0.20	0.23	0.23	5.70	9.07	9.22
	σ_{ij}^{-}	0.46	0.06	0.21	0.48	0.07	0.23	4.54	10.52	7.83
Shear	σ_{ij}^{+}	0.20	0.36	0.24	0.20	0.37	0.24	3.43	1.99	2.82
	σ_{ij}^{-}	0.46	0.12	0.24	0.47	0.12	0.25	3.33	2.85	3.20

Case 5: Targeted recycled fibers index: RI= 50%

Load case	**Stress**	***Eff*$_{11}$**	***Eff*$_{22}$**	***Eff*$_{12}$**	***Eff*$_{11}$**	***Eff*$_{22}$**	***Eff*$_{12}$**	**Δ*Eff*$_{11}$**	**Δ*Eff*$_{22}$**	**Δ*Eff*$_{12}$**
		Reference RI=0%			**RI= 50%**					
Unit	-	-	-	-	-	-	-	%	%	%
Bending	σ_{ij}^{+}	0.19	0.18	0.17	0.20	0.19	0.17	3.65	3.65	0.43
	σ_{ij}^{-}	0.45	0.06	0.17	0.47	0.06	0.16	3.63	5.89	-6.55
Tensile	σ_{ij}^{+}	0.22	0.45	0.27	0.24	0.48	0.28	6.90	5.80	7.09
	σ_{ij}^{-}	0.14	0.03	0.27	0.15	0.04	0.29	12.03	16.40	7.42
Torsion	σ_{ij}^{+}	0.19	0.21	0.21	0.20	0.24	0.24	5.79	14.38	12.23
	σ_{ij}^{-}	0.46	0.06	0.21	0.48	0.07	0.24	5.39	9.94	12.30
Shear	σ_{ij}^{+}	0.20	0.36	0.24	0.21	0.38	0.23	5.59	5.11	-2.63
	σ_{ij}^{-}	0.46	0.12	0.24	0.48	0.13	0.25	4.94	6.06	6.45

Results for the **hat-stiffener with skin** at three different efforts for four loading cases of five tests cases with an increasing recycling index from 10 % to 50 %

Case 1: Targeted recycled fibers index: RI= 10%

Load case	Stress	Eff_{11}	Eff_{22}	Eff_{12}	Eff_{11}	Eff_{22}	Eff_{12}	ΔEff_{11}	ΔEff_{22}	ΔEff_{12}
		Reference RI=0%			RI= 10%					
Unit	-	-	-	-	-	-	-	%	%	%
Bending	σ_{ij}^{+}	0.23	0.45	0.21	0.23	0.45	0.21	0.00	0.00	0.00
	σ_{ij}^{-}	0.16	0.04	0.21	0.16	0.04	0.21	0.00	0.00	0.00
Tensile	σ_{ij}^{+}	0.19	0.37	0.23	0.19	0.37	0.23	0.00	0.00	0.00
	σ_{ij}^{-}	0.45	0.11	0.23	0.45	0.11	0.23	0.00	0.00	0.00
Torsion	σ_{ij}^{+}	0.23	0.45	0.29	0.23	0.45	0.29	0.43	0.50	0.31
	σ_{ij}^{-}	0.11	0.05	0.27	0.12	0.05	0.27	0.36	0.00	0.05
Shear	σ_{ij}^{+}	0.19	0.36	0.28	0.20	0.38	0.31	7.19	3.02	10.92
	σ_{ij}^{-}	0.46	0.09	0.29	0.47	0.09	0.30	3.54	2.68	3.07

Case 2: Targeted recycled fibers index: RI= 20%

Load case	Stress	Eff_{11}	Eff_{22}	Eff_{12}	Eff_{11}	Eff_{22}	Eff_{12}	ΔEff_{11}	ΔEff_{22}	ΔEff_{12}
		Reference RI=0%			RI= 20%					
Unit	-	-	-	-	-	-	-	%	%	%
Bending	σ_{ij}^{+}	0.23	0.45	0.21	0.23	0.45	0.22	0.25	0.05	0.98
	σ_{ij}^{-}	0.16	0.04	0.21	0.16	0.04	0.22	0.26	0.28	0.91
Tensile	σ_{ij}^{+}	0.19	0.37	0.23	0.19	0.38	0.23	0.13	0.16	-0.13
	σ_{ij}^{-}	0.45	0.11	0.23	0.46	0.11	0.23	0.18	0.17	0.39
Torsion	σ_{ij}^{+}	0.23	0.45	0.29	0.24	0.46	0.29	1.45	1.90	0.16
	σ_{ij}^{-}	0.11	0.05	0.27	0.12	0.05	0.27	0.36	-0.08	0.88
Shear	σ_{ij}^{+}	0.19	0.36	0.28	0.20	0.40	0.31	6.63	10.35	12.05
	σ_{ij}^{-}	0.46	0.09	0.29	0.48	0.09	0.31	4.58	1.90	6.08

Case 3: Targeted recycled fibers index: RI= 30%

Load case	Stress	Eff_{11}	Eff_{22}	Eff_{12}	Eff_{11}	Eff_{22}	Eff_{12}	ΔEff_{11}	ΔEff_{22}	ΔEff_{12}
		Reference RI=0%			RI= 30%					
Unit	-	-	-	-	-	-	-	%	%	%
Bending	σ_{ij}^{+}	0.23	0.45	0.21	0.23	0.45	0.21	0.08	-0.09	0.42
	σ_{ij}^{-}	0.16	0.04	0.21	0.16	0.04	0.21	-0.26	-0.27	0.35
Tensile	σ_{ij}^{+}	0.19	0.37	0.23	0.19	0.38	0.23	0.20	0.16	0.13
	σ_{ij}^{-}	0.45	0.11	0.23	0.46	0.11	0.23	0.58	0.56	0.51
Torsion	σ_{ij}^{+}	0.23	0.45	0.29	0.23	0.45	0.29	0.87	0.86	0.63
	σ_{ij}^{-}	0.11	0.05	0.27	0.12	0.05	0.27	0.89	-0.08	0.44
Shear	σ_{ij}^{+}	0.19	0.36	0.28	0.20	0.37	0.31	5.00	2.35	11.14
	σ_{ij}^{-}	0.46	0.09	0.29	0.47	0.09	0.32	2.20	3.66	7.87

Case 4: Targeted recycled fibers index: RI= 40%

Load case	Stress	Eff_{11}	Eff_{22}	Eff_{12}	Eff_{11}	Eff_{22}	Eff_{12}	ΔEff_{11}	ΔEff_{22}	ΔEff_{12}
		Reference RI=0%			RI= 40%					
Unit	-	-	-	-	-	-	-	%	%	%
Bending	σ_{ij}^{+}	0.23	0.45	0.21	0.23	0.46	0.22	1.56	1.49	1.53
	σ_{ij}^{-}	0.16	0.04	0.21	0.16	0.04	0.22	2.12	2.16	1.95
Tensile	σ_{ij}^{+}	0.19	0.37	0.23	0.20	0.38	0.23	1.53	1.47	1.81
	σ_{ij}^{-}	0.45	0.11	0.23	0.46	0.11	0.23	0.65	0.61	0.71
Torsion	σ_{ij}^{+}	0.23	0.45	0.29	0.24	0.46	0.29	2.38	2.49	1.78
	σ_{ij}^{-}	0.11	0.05	0.27	0.12	0.05	0.28	2.67	0.38	3.45
Shear	σ_{ij}^{+}	0.19	0.36	0.28	0.21	0.39	0.34	12.81	8.23	21.41
	σ_{ij}^{-}	0.46	0.09	0.29	0.48	0.10	0.35	5.76	12.76	18.60

Case 5: Targeted recycled fibers index: RI= 50%

Load case	Stress	Eff_{11}	Eff_{22}	Eff_{12}	Eff_{11}	Eff_{22}	Eff_{12}	ΔEff_{11}	ΔEff_{22}	ΔEff_{12}
		Reference RI=0%			RI= 50%					

Unit	-	-	-	-	-	-	-	%	%	%
Bending	σ_{ij}^{+}	0.23	0.45	0.21	0.23	0.46	0.22	2.70	2.49	2.51
	σ_{ij}^{-}	0.16	0.04	0.21	0.16	0.04	0.22	0.45	0.99	2.44
Tensile	σ_{ij}^{+}	0.19	0.37	0.23	0.20	0.38	0.23	0.89	0.93	0.58
	σ_{ij}^{-}	0.45	0.11	0.23	0.46	0.11	0.24	1.44	1.44	1.16
Torsion	σ_{ij}^{+}	0.23	0.45	0.29	0.24	0.46	0.29	2.42	2.58	2.30
	σ_{ij}^{-}	0.11	0.05	0.27	0.12	0.05	0.28	2.58	0.08	1.32
Shear	σ_{ij}^{+}	0.19	0.36	0.28	0.21	0.39	0.34	9.74	7.22	21.73
	σ_{ij}^{-}	0.46	0.09	0.29	0.48	0.10	0.33	5.25	12.40	13.34